PHYSICAL REVIEW VOLUME 67, NUMBERS 11 AND 12 JUNE 1 AND 15, 1945

Theoretical Continuous X-Ray Energy and Polarization

PAUL KIRKPATRICK AND LUCILLE WIEDMANN
Stanford University, Stanford University, California

(Received April 2, 1945)

By the theory of Sommerfeld, relativity effects and retardation of potential being neglected, matrix elements and associated components of continuous spectrum x-radiation are computed for a variety of electron-nucleus collisions and for a distributed series of positions in the spectrum. The calculations cover values of V/Z^2 from 0.06128 to 3.356, where Z is the atomic number of the nucleus, and V is the bombardment potential in electrostatic units. Accuracy of calculation is 1 percent. Screening is neglected except at the long wave limit of the spectra where it is taken into account by Sauter's method. Empirical algebraic formulas are found which closely represent the rigorously calculated results. Intensity and polarization predictions for any direction of emission and any excitation conditions within the range of applicability of the theory may be readily drawn from the computed results. Elwert's proposed correction factor for rectifying the approximate spectral intensities of Sommerfeld and Maue is found effective within the limits of its restricting assumptions. Theoretical efficiencies of continuous x-ray production are calculated by combining theoretical intensities with known rates of electron energy loss in traversing matter. Thick target efficiency (a ratio, not percent) is given by $1.4\times10^{-6}Z$ kv. Thin target efficiency is found to be approximately twice the thick target efficiency for any given Z and kv.

THE problem of the continuous x-ray spectrum is to find answers to such questions as the following: When an electron of stated kinetic energy collides with a thin layer of matter of atomic number Z and of some given surface density, what is the probability that a photon whose frequency lies between any stipulated limits shall be emitted in an elementary solid angle of specified magnitude oriented in any defined manner with respect to the direction of motion of the bombarding electron? A further question concerns the state of polarization of such a photon.

Answers to these questions are implicit in extant theory, but in only a very few cases have explicit numerical answers been extracted from the theories and placed on the record. It is not yet possible to say broadly that the theory either does or does not agree with experimental facts, though a few encouraging similarities have appeared. We shall not have a satisfying number of such comparisons without further work on both sides of the gap, i.e., until many more good measurements have been completed and until theoretical predictions are made available *in numerical form*.

The present paper attempts to supply the second of these necessities. It contributes nothing to the basic theoretical picture according to which the emission of the continuous x-ray spectrum is now understood; rather, it presents a computational procedure for obtaining numerical values of x-ray energy and polarization from the theory, together with the results of such calculations.

For a system consisting of a bare nucleus and one electron, Schrödinger's equation predicts a continuous range of *positive* energy states, and a continuous spectrum must result from the joint operation of the possible transitions between such states. The spectral features may be deduced, as Oppenheimer[1] and Sugiura[2] have shown, by calculating matrix elements from characteristic functions corresponding to states involved in the transitions, but the method introduced by Sommerfeld[3] and developed by a number of subsequent theorists has greater analytical simplicity and will be followed in the present paper.

The theory of Sommerfeld considers the wave systems of an electron approaching an atomic nucleus and departing with altered direction and reduced speed, having suffered an energy loss which appears as the energy of the emitted photon. The single process can be described with rigor, but the integration over all possible direc-

[1] J. R. Oppenheimer, Zeits. f. Physik **55**, 725 (1929).
[2] Y. Sugiura, Sci. Pap. Inst. Phys. Chem. Res. Tokyo **17**, 89 (1931); and earlier contributions referred to therein.
[3] A. Sommerfeld, Ann. d. Physik [5] **11**, 257 (1931); O. Scherzer, Ann. d. Physik [5] **13**, 137 (1932); F. Sauter, Ann. d. Physik [5] **18**, 486 (1933), [5] **20**, 404 (1934); A. Sommerfeld and A. W. Maue, Ann. d. Physik [5] **23**, 589 (1935); G. Elwert, Ann. d. Physik [5] **34**, 178 (1939); R. Weinstock, Phys. Rev. **61**, 585 (1942), **65**, 1 (1944).

tions of departure of the electron—a necessary operation if theory is to be compared with experiment—has been found troublesome by all who have tried it.

Approximations, physical or mathematical, have been necessary features of all the treatments. The present results are conditioned by the inexact physical assumptions of the original Sommerfeld[3] theory, but we follow Weinstock[3] in avoiding mathematical approximations such as those which restricted the applicability of the results of Sauter and of Elwert.[4]

The questionable physical assumptions and approximations are the following: (a) Except in connection with the long wave limit of the spectrum, atomic electrons are ignored, and the nucleus is assumed to be the center of a pure Coulomb field. (b) Relativity effects, retardation of potential, and the effects of electron spin are neglected. (c) The de Broglie waves of the approaching and receding electron are treated as plane waves, filling all space.

Picture a row of electrons moving along or closely parallel to the x-axis of a cartesian coordinate system (see Fig. 8), approaching the origin from the negative side with speed v_1 conferred by a potential difference V. Upon arriving at the origin, the electrons strike or pass through a plane target coinciding with the yz-plane which is composed of atoms of atomic number Z in a uniform distribution. We investigate the continuous x-radiation resulting from collisions at the origin and departing in a direction lying in the xz-plane and making an angle θ with the positive x-direction. The electron leaves the collision with speed v_2. As applied to such a picture, the theory deals in probabilities of photon emission, but with large numbers of atoms or of electrons, such probabilities increase proportionately, and one may speak with statistical accuracy of emitted intensities, powers, and energies.

The bombarded and emitting atoms simulate a source possessing calculable component Hertzian dipole moments, each of which produces radiation components I_x, I_y, and I_z, proportional to the square of the corresponding moment. The total intensity proceeding in a direction θ consists in general of contributions from all three radiation components weighted with reference to the angles between their dipole axes and the direction of observation. The observable intensity is given by[5]

$$I_\theta = I_x \sin^2\theta + I_y + I_z \cos^2\theta. \tag{1}$$

The calculation and discussion of $I_{x,y,z}$ are the objects of this paper; these components will be defined in such a way that I_θ (not rigorously a radiation intensity) comes out in the units ergs per steradian per unit frequency range per bombarding electron per atom-per-square-centimeter of target area. Neglect of electron spin leaves the direction of bombardment an axis of complete symmetry, so $I_y = I_z$ necessarily. There remain two quantities, I_x and I_y, to calculate, and each is a function of the four parameters θ, V, Z, and the frequency ν, a group which will be found reducible to three. In terms of these components, the intensity and polarization of radiation emitted in the direction θ are given by

$$\left.\begin{aligned} I_\theta &= I_x \sin^2\theta + I_y(1+\cos^2\theta) \\ \mathcal{I}_\theta &= \frac{1-(I_y/I_x)}{1+(I_y/I_x)(2\csc^2\theta-1)} \end{aligned}\right\}. \tag{2}$$

The method of Sommerfeld yields:

$$I_{x,y,z} = \frac{4\pi e^6 Z^2 (Ve-h\nu) N^2_{x,y,z}}{[1-\exp(-4\pi^2 e^2 Z/v_2 h)][\exp(4\pi^2 e^2 Z/v_1 h)-1][(Ve)^{\frac{1}{2}}-(Ve-h\nu)^{\frac{1}{2}}]^4 mc^3}, \tag{3}$$

where $N^2_{x,y,z}$ are dimensionless quantities equivalent to $M^2_{x,y,z}/|A|^2$ of Weinstock's first reference. The computation of these quantities is almost the whole of the problem confronting the computer.

[4] Sauter is limited by Born's first approximation, $Ze^2/\hbar v_{1,2} \ll 1$; while Elwert's method is restricted by the assumption $(Ze^2/\hbar v_2)-(Ze^2/\hbar v_1) \ll 1$ or $Ze^2/\hbar v_1 \ll 1$. The effects of these conditions will be noted on a subsequent page.

CALCULATION OF N_y^2 $(=N_z^2)$

From Weinstock's derivation one finds

$$N_y^2 = \frac{16\pi^3 Z^2 e^3 m}{h^2 V \xi_0^3}\left[1+\frac{2\pi^2 Z^2 e^4 m}{h^2(Ve-h\nu)}\right] \times \int_0^{w_0}\left\{\frac{\xi_0 w}{1-w}+\frac{w^2}{(1-w)^2}\right\}|G_3|^2 dw. \tag{4}$$

[5] G. Elwert, reference 3; p. 194.

New symbols appearing in Eq. (4) are defined as follows:

$$\xi_0=-4n_1n_2/(n_1-n_2)^2, \quad w_0=\xi_0/(\xi_0-1).$$

The quantity G_3 is the hypergeometric function $F(1+n_1, -n_2, 2, w)$ where n_1 and n_2 are imaginary quantities defined by $n_{1,2}=(-2\pi e^2Zi)/(hv_{1,2})$. The physical significance of w is of no concern since it goes out in the definite integration.

Weinstock expanded G_3 in series and integrated Eq. (4) term by term, obtaining his compact Eq. (9). Although this works well in some cases, it has not been found generally trustworthy because of the danger that the series of integrals may be chopped off too soon. It is quite impossible to depend upon appearances in estimating the progress of its convergence, and no positive criterion has been found. It is known that as many as twenty terms are insufficient in certain cases to reduce the residue to negligibility, so the evaluation is both suspect and laborious. It was decided, therefore, to evaluate the integrand in Eq. (4) for representative values of w and to carry out the integration graphically.

The range of integration extends from zero to w_0, a positive quantity lying between zero and unity. For those cases (values of V and ν) which give values of w_0 not too near to unity, say not exceeding 0.75, the necessary values of G_3 may be obtained from the standard hypergeometric expansion

$$F(a, b, c, x)\equiv 1+\frac{abx}{1c}+\frac{a(a+1)b(b+1)x^2}{1\cdot 2\cdot c(c+1)}+\frac{a(a+1)(a+2)b(b+1)(b+2)x^3}{1\cdot 2\cdot 3\cdot c(c+1)(c+2)}+\cdots\equiv\sum_{\mu=0}^{\mu=\infty}g_\mu x^\mu$$

where μ is an integer designating a series term, which starts with $\mu=0$ for the first term. The coefficients are given by

$$g_0=1, \text{ and in general}$$

$$g_{\mu+1}=\frac{(\mu+a)(\mu+b)}{(\mu+1)(\mu+c)}g_\mu.$$

By use of this series, G_3 may usually be evaluated with an uncertainty not greater than one percent without going beyond 10 or 15 terms. For values of w too large for prompt convergence, use is made of the identity[6]

$$G_3=C_1F(1+n_1, -n_2, n_1-n_2, 1-w)+C_2F(1-n_1, 2+n_2, 2-n_1+n_2, 1-w),$$

where

$$C_1=\frac{-n_1+n_2}{-n_1n_2(1+n_2)}\bar{\Delta},$$

$$C_2=\frac{\Delta}{n_1(-1+n_1-n_2)}(1-w)^{1-n_1+n_2},$$

$$\Delta=\Gamma(n_1-n_2)/\Gamma(n_1)\Gamma(-n_2),$$

and $\bar{\Delta}$ designates the complex conjugate of Δ.

Numerical evaluation of Δ is most readily carried out by means of the identity

$$1/\Gamma(x)=x(x+1)\times(1+B_1x+B_2x^2+B_3x^3+\cdots). \quad (5)$$

The coefficients of x as calculated by Bourguet[7] are reproduced in Table I.

The terms in the series of Eq. (5) are alternately imaginary and real, leading to a complex Δ. For the largest values of n_2, the tabulated coefficients are insufficient, and it is advantageous to use Legendre's duplication formula

$$\pi^{\frac{1}{2}}\Gamma(2x)=2^{2x-1}\Gamma(x)\Gamma(x+\tfrac{1}{2}),$$

to bring the arguments of the gamma-functions within the range of the table. The imaginary character of n_1 and n_2 requires special attention in the evaluation of C_2; here we may write

$$(1-w)^{1-n_1+n_2}=(1-w)(\cos\theta+i\sin\theta),$$

in which

$$\theta=|n_1-n_2|\log(1/1-w).$$

If the integrand of Eq. (4) be plotted as a function of w, the curve will usually be found inconvenient for planimeter integration because of the high and narrow peak at the upper limit. This feature is avoided by plotting as a function

[6] E. T. Copson, *An Introduction to the Theory of Functions of a Complex Variable* (Oxford University Press, New York, 1935), p. 251.

[7] L. Bourguet, Acta Math. 2, 261 (1883). Harold T. Davis, *Tables of the Higher Mathematical Functions* (The Principia Press, Inc., Bloomington, Indiana, 1933), Vol. 1, p. 185.

of u, where $u=1/(1-w)$, in which case the errors of area measurement may well be less than those of computation. The transformed integral is

$$\int_1^{1-\xi_0} \frac{(u-1)(\xi_0+u-1)}{u^2}|G_3|^2 du.$$

As ξ_0 increases, the maximum of the integrand becomes higher and narrower, but plotting in two or three different sections with suitable changes of scale readily keeps it in hand.

CALCULATION OF N_x^2

The calculation of N_x^2 might be carried out in a manner analogous to that described above, but Weinstock's expression contains three definite integrals, and although he has shown how to replace them by infinite series, the problem of convergence persuades us to adopt a differing approach. Sommerfeld and Maue have shown how to express the sum $N^2=N_x^2+N_y^2+N_z^2$ in closed form, and Weinstock has put their expression into a form based upon four rapidly converging series, two of which we find to be identical. We therefore employ Weinstock's equation for N^2 in the form shown below and later solve for $N_x^2=N^2-2N_y^2$. This avoidance of a direct attack upon N_x^2 follows, in principle, the example of Elwert.

TABLE I. Coefficients in the power-series expansion

$$\frac{1}{\Gamma(x)}=x(x+1)(1+B_1x+B_2x^2+\cdots).$$

n	B_n			
1	−0.4227	8433	5098	4671
2	−0.2330	9373	6421	7867
3	0.1910	9110	1387	6915
4	−0.0245	5249	0005	4000
5	−0.0176	4524	4550	1443
6	0.0080	2327	3022	2673
7	−0.0008	0432	9775	6044
8	−0.0003	6083	7816	2548
9	0.0001	4559	6142	1399
10	−0.0000	1754	5859	7517
11	−0.0000	0258	8995	0224
12	0.0000	0133	8501	5466
13	−0.0000	0020	5474	3152
14	−0.0000	0000	0159	5268
15	0.0000	0000	6275	6218
16	−0.0000	0000	1273	6143
17	0.0000	0000	0092	3397
18	0.0000	0000	0012	0028
19	−0.0000	0000	0004	2202
20	0.0000	0000	0000	5240
21	−0.0000	0000	0000	0140
22	−0.0000	0000	0000	0067

The working equation for N^2 is

$$N^2=\frac{-16\pi}{\xi_0}\left[\left|\frac{\Delta}{n_1}\right|^2\sum_{r=1}^{\infty} rq_r\xi_0^{-r-1} - \Re\left\{\frac{\Delta^2}{n_1n_2}(-\xi_0)^{n_1-n_2}\left[\sum_{r=1}^{\infty} rj_r\xi_0^{-r-1} - (n_1-n_2)\sum_{r=0}^{\infty} j_r\xi_0^{-r-1}\right]\right\}\right], \quad (6)$$

wherein $\Re\equiv$"real part of," and the quantities q_r and j_r are themselves defined by the finite series:

$$q_r=\sum_{\nu=0}^{r} g_{4,\nu}g^*_{4,r-\nu}; \quad j_r=\sum_{\nu=0}^{r} g_{4,\nu}g^*_{5,r-\nu}.$$

Quantities in these series are defined and calculated by the recursion relations:

$$g_{4,0}=g_{5,0}=1,$$

$$g_{4,\nu}=\frac{(\nu-1-n_1)^2}{\nu(\nu+n_2-n_1)}g_{4,\nu-1},$$

$$g_{5,\nu}=\frac{(\nu-1-n_2)^2}{\nu(\nu+n_1-n_2)}g_{5,\nu-1}.$$

The asterisk (*) denotes the conjugate function. In these series ν and r are real integers assuming consecutive values within the stated ranges. The convergence is such that as few as three terms sometimes suffice to fix the value of a series. The g's are, of course, complex, but the conjugates in q_r and j_r cancel out the imaginaries and leave these quantities and their series real.

NUMERICAL EVALUATION

Inspection of the foregoing equations shows that the variables V, Z, and ν are present only in combinations reducible to V/Z^2 and ν/ν_0. This reduction of the number of parameters controlling the spectral features from four to three (the two quotients above and θ) greatly reduces the amount of computation necessary to cover the full range of experimental variables, since any one complete calculation furnishes a separate prediction concerning each of the 92 elements.

TABLE II. Components and total energy of radiation.

V/Z^2	ν/ν_0	$I_x\times10^{50}$	$I_y(=I_z)\times10^{50}$	$W\times10^{50}$	V/Z^2	ν/ν_0	$I_x\times10^{50}$	$I_y(=I_z)\times10^{50}$	$W\times10^{50}$
3.356	0.403	0.0809	0.0296	1.17	0.06041	1.00	5.51	0.718	58.2
						0.624	5.12	1.35	65.4
2.171	0.623	0.128	0.0228	1.45		0.443	4.86	1.79	70.6
						0.217	4.40	2.81	83.9
1.776	1.00	0.146	0.00132	1.24		0.00	1.72	5.81	112.0
	0.761	0.154	0.016	1.56					
	0.197	0.144	0.105	2.97	0.03776	1.00	8.48	1.30	92.9
	0.0962	0.136	0.151	3.67		0.708	8.11	1.92	100.0
	0.00	0.0586	0.223	4.23		0.346	7.34	3.32	117.0
						0.00	2.78	9.10	176.0
1.351	1.00	0.207	0.00223	1.77					
					0.03546	1.00	9.00	1.40	98.9
0.7896	1.00	0.398	0.00761	3.47		0.761	8.73	1.92	105.0
	0.624	0.377	0.072	4.37		0.197	7.35	4.76	141.0
	0.443	0.361	0.121	5.05		0.0962	6.75	6.34	163.0
	0.217	0.332	0.227	6.59		0.00	2.95	9.60	186.0
	0.00	0.132	0.496	9.42					
					0.02723	1.00	11.5	1.92	128.0
0.4934	1.00	0.685	0.0191	6.06		0.624	10.8	3.01	141.0
	0.708	0.637	0.0948	6.92		0.443	10.4	3.84	152.0
	0.346	0.578	0.254	9.10		0.217	9.74	5.68	177.0
	0.00	0.211	0.776	14.8		0.00	3.81	12.2	236.0
0.3493	1.00	0.999	0.0378	9.01	0.02265	1.00	13.62	2.37	154.0
						0.577	12.73	3.81	171.0
0.2961	1.00	1.20	0.0518	10.9		0.00	4.60	14.5	282.0
	0.577	1.05	0.250	13.0					
	0.00	0.351	1.26	24.1	0.01702	1.00	17.7	3.27	204.0
						0.708	17.2	4.31	216.0
0.1709	1.00	2.12	0.141	20.1		0.346	16.0	6.84	248.0
						0.00	6.09	18.8	366.0
0.1359	1.00	2.63	0.214	25.6					
	0.761	2.43	0.402	27.1	0.01576	1.00	19.0	3.58	219.0
	0.197	1.91	1.39	39.3		0.624	18.2	5.14	238.0
	0.0962	1.79	1.90	46.8		0.443	17.7	6.36	255.0
	0.00	0.765	2.705	51.7		0.217	16.6	9.25	294.0
						0.00	6.58	20.2	394.0
0.06128	1.00	5.43	0.697	57.2					
	0.761	5.18	1.05	61.0	0.009854	0.708	28.9	7.48	368.0
	0.197	4.26	2.92	84.5		0.346	27.2	11.2	415.0
	0.0962	3.92	3.95	99.0		0.00	10.5	30.5	599.0
	0.00	1.70	5.74	111.0					

Many of these predictions, however, relate to definitely relativistic voltage or frequency ranges and are, therefore, not fully applicable.

Values of I_x and $I_y=I_z$, calculated by the methods described above are listed in Table II, along with the related values of V/Z^2 and ν/ν_0. Birge's[8] 1941 values of the atomic constants have been used. Since the I's vary approximately as the ninth power of e, precision here is not as superfluous as might be assumed. Indeed, an error in e as great as the discrepancy between today's value and that of a decade ago could easily throw the calculated intensities off by much more than the errors of intensity measurement.

[8] R. T. Birge, Rev. Mod. Phys. **13**, 233 (1941).

The quantity W, introduced in the fifth and last columns of Table II, is the total energy of continuous x-radiation in all directions. Integration of I_θ of Eq. (2) over the 4π steradians of space surrounding the point of collision gives at once $W=(8\pi/3)[I_x+I_y+I_z]$, a function of ν given in the units ergs per unit frequency interval per bombarding electron per atom-per-square-centimeter of target area.

The numerical values in Table II have been checked against each other by many graphical tests, and indeed, such checks were used at all stages of the calculations as a guard against errors of computation. Although each row of the table (except at $\nu/\nu_0=0$ and some at $\nu/\nu_0=1$) represents over 1200 elementary computing operations, it is believed that computing errors

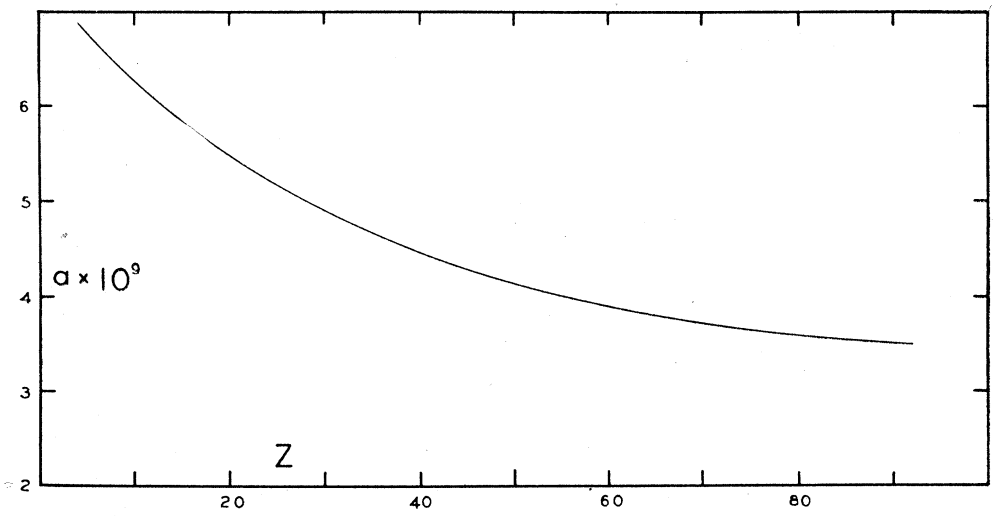

FIG. 1. Screening constants a (in cm) of the Sauter atomic potential distribution $V_s=(-eZ/r)\exp(-r/a)$. Values shown by curve give best agreement with Fermi atomic potentials.

and approximations have in no case impaired a calculated result by more than one percent.

Low Frequency Limit

The computations described above have been subject to the assumption that the bombarded nucleus is effectively unscreened. This does not preclude the application of the results to real nuclei,[9] fully clothed with screening electrons, as long as the acceleration of the bombarding electrons takes place inside of the surrounding electron screen. This is probably what happens in the production of most of the spectrum, but it definitely does not always happen when radiation of vanishingly small quantum energy is emitted. Such radiation requires the application of such slight forces to the bombardment electron that it may be produced by an electron passing a bare nucleus at a great distance. The collision cross section for radiation of zero frequency is very great, and one readily sees why the Sommerfeld theory predicts infinite intensity at $\lambda=\infty$. At this end of the spectrum, it is necessary to assume some screening if predictions applicable to real atoms are desired.

We have, therefore, calculated $I_{x,y}$ at $\nu=0$ by the method of Sauter, who shows how to compute the radiation from an atom whose potential distribution is given by $V_S=(-eZ/r)\exp(-r/a)$, where r is a radial coordinate originating at the atomic nucleus. In the unscreened case ($a=\infty$), Sauter's method gives intensity values which are much too low in the high frequency region of the spectrum, but Elwert has shown that Sauter's method agrees with the Sommerfeld method in

TABLE III. Radiation components at $\nu=0$ for screened nuclei.

V	Z	$I_x\times10^{60}$	$I_y\times10^{60}$	V	Z	$I_x\times10^{60}$	$I_y\times10^{60}$
28.43	4	.0584	.190	33.99	30	2.77	8.14
44.40	5	.0585	.199	48.94	36	2.78	8.45
87.03	7	.0586	.217	83.40	47	2.78	8.93
143.9	9	.0586	.230	131.4	59	2.78	9.34
214.9	11	.0586	.240	201.2	73	2.79	9.78
300.2	13	.0586	.248	299.1	89	2.79	10.2
28.42	6	.131	.418	300.2	92	2.93	10.8
50.54	8	.132	.451				
78.96	10	.132	.476	33.36	35	3.80	11.1
133.4	13	.132	.504	50.34	43	3.81	11.6
202.1	16	.132	.527	82.36	55	3.81	12.2
315.8	20	.132	.544	133.4	70	3.81	12.8
				201.4	86	3.82	13.4
31.58	8	.210	.673	230.5	92	3.82	13.6
49.34	10	.211	.713				
83.40	13	.211	.758	50.04	47	4.57	2.99
142.6	17	.211	.803				
197.3	20	.211	.828	32.95	44	6.07	17.2
308.4	25	.211	.864	49.64	54	6.08	18.0
				83.40	70	6.09	19.1
50.04	13	.351	1.17	144.0	92	6.10	20.3
34.76	16	.763	2.39	33.36	46	6.56	18.6
49.07	19	.764	2.47	49.44	56	6.57	19.4
84.93	25	.765	2.65	84.00	73	6.58	20.6
139.1	32	.765	2.77	133.4	92	6.59	21.8
206.7	39	.765	2.87				
300.2	47	.766	2.97	33.15	58	10.5	28.7
				49.67	71	10.5	30.3
300.2	70	1.70	6.36	83.40	92	10.5	32.3
34.79	24	1.72	5.21				
50.80	29	1.72	5.46				
82.69	37	1.72	5.73				
133.4	47	1.72	5.98				
203.2	58	1.72	6.21				
296.0	70	1.72	6.44				

[9] A. L. Hughes, Phys. Rev. **55**, 350 (1939), shows that atomic electrons play a negligible part in the *elastic* scattering of fast electrons by atoms.

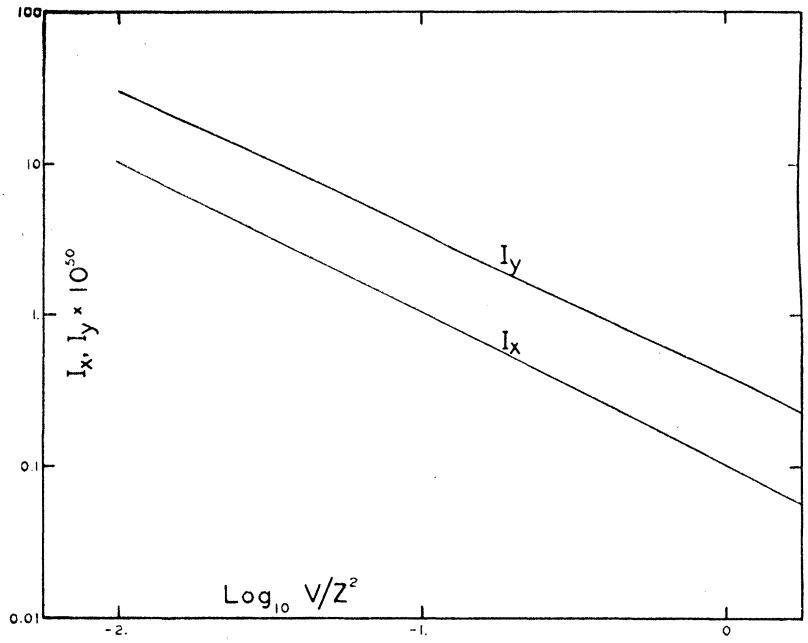

FIG. 2. Radiation components from Table II at the long wave limit ($\nu=0$). (Note both axes are logarithmic.) $I_y > I_x$ means negative polarization.

its approach to infinite intensities at the low frequency limit. It seems reasonable therefore, to seek a proper value of a and apply the method at the long wave limit.

The values of a adopted were those which brought the Sauter potential distribution into best agreement with the Fermi[10] atomic potential $V_F = Ze\varphi/r$ over the region of r for which the Fermi expression is defined. Figure 1 shows the variation of a with Z.

Equation (20) of Sauter's[11] first paper may be specialized for $\nu=0$ and decomposed into

$$\left.\begin{aligned} I_x &= \frac{e^5}{c^3 m(V/Z^2)}\left[\frac{-2\hbar^2}{8mVea^2}\log\frac{8mVea^2}{\hbar^2}+1\right] \\ I_y &= \frac{e^5}{c^3 m(V/Z^2)} \\ &\quad\times\left[\left(\frac{1}{2}+\frac{\hbar^2}{8mVea^2}\right)\log\frac{8mVea^2}{\hbar^2}-1\right] \end{aligned}\right\}. \quad (7)$$

These values of I_x and I_y are not functions of V/Z^2 alone but depend also upon V. This dependence is very slight for I_x, a variation of V by a factor of 10 (V/Z^2 remaining constant) affecting I_x by much less than one percent. In the case of I_y, the corresponding variation goes as high as 25 percent. The difference is classically understandable since the force between a nucleus and a remote passing electron is principally in the component lying along the impact parameter. In plotting spectral features as functions of V/Z^2 and ν/ν_0, we have in some cases to follow used mean values of the low frequency limit I_x and I_y within the narrow scatter described above. Such mean values are entered in Table II, and Table III contains a fuller display of all the separate values calculated from Eqs. (7). These easily calculated values (Fig. 2) are in every case readily acceptable extensions of our hard-won curves for finite frequencies.

High Frequency Limit

No short cut is available for computing the short wave limit radiation components. The elaborate methods described above are applicable, but several of the series must be carried out to tedious lengths. The second reference of

[10] E. Fermi, Zeits. f. Physik **48**, 73 (1928). The quantities ϵ and φ are defined and tabulated in this paper.

[11] There are two mistakes in the equation as printed: R^0 should be R^2, and p_0 in the denominator outside the braces should be 3.

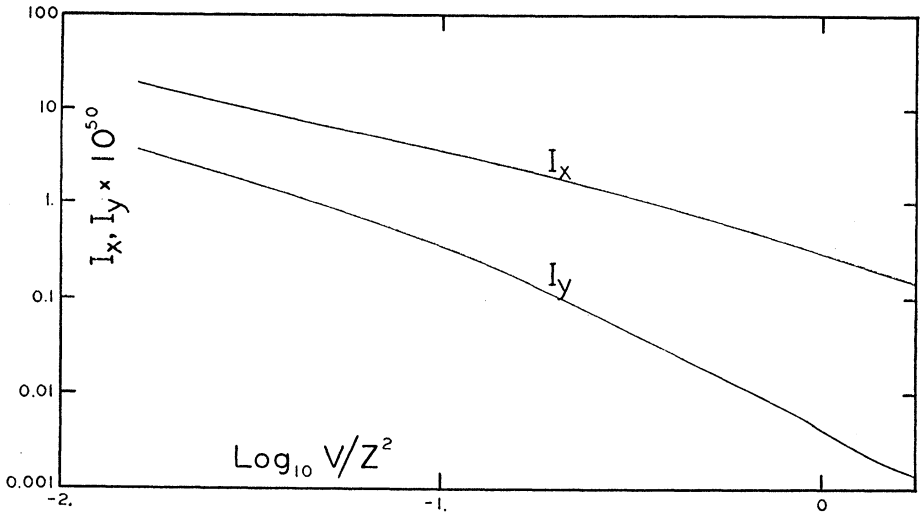

FIG. 3. Radiation components from Table II at the short wave limit ($\nu=\nu_0$). (Note both axes are logarithmic.)

Weinstock indicates the special forms which the working equations take at this limit, but no overall simplification results. We have, therefore, carried out the computations for only four cases at the limit. These have been supplemented by limit data obtained by extrapolation of results of related cases for which $\nu/\nu_0<1$. Since the radiation components are functions of two variables (V/Z^2 and ν/ν_0), it was possible to arrive at the same result by two quite independent extrapolations. If two such extrapolations yielded results in agreement to within one percent, the result was accepted as correct. Figure 3 shows the variation of I_x and I_y at the high frequency limit. These curves are important in their relation to the mooted question of high frequency limit polarization.

Approximate Representation

Detailed inspection of Table II shows that the values of I_x and I_y are, to a rough approximation, inversely proportional to V/Z^2. For I_x the approximation is close enough so that all the values within the range of our investigation may be stated with a mean error of 10 percent and a maximum error of 20 percent by the equation

$$I_x=3.0\times10^{-51}Z^2/V.$$

Near the short wave limit ($\nu/\nu_0=1$), the variation of I_x with V/Z^2 is not as simple, and the maximum errors are found. Far from the short wave limit, approximate representations become quite satisfactory; all values of I_x investigated at $\nu/\nu_0=0.2$ are given by $I_x=2.6\times10^{-51}Z^2/V$ with errors all under 2 percent. It should be realized that the word "error" as used here means only the discrepancy between the approximate expression and the more rigorously calculated values of Table II; it has no relation either to the errors of the Sommerfeld theory or the errors of computation.

The values of I_y and I_z are less easily summarized. They increase rapidly with increasing wave-length in a given spectrum whereas the general (but not invariable) tendency of I_x is to decrease slowly. At $\nu/\nu_0=0.4$ all values of $I_y(=I_z)$ are given with errors under 6 percent by the expression $1.1\times10^{-51}Z^2/V$, but elsewhere in the spectra, expressions of this type do not suffice.

In view of the enormous amount of work involved in computing spectral characteristics from the Sommerfeld equations or any of their modifications, it seems worth while to consider a second approximate representation of their results. Using primes to distinguish these approximations, we find:

$$I_x'\times10^{50}V/Z^2=0.252+a(\nu/\nu_0-0.135)-b(\nu/\nu_0-0.135)^2, \quad (8)$$

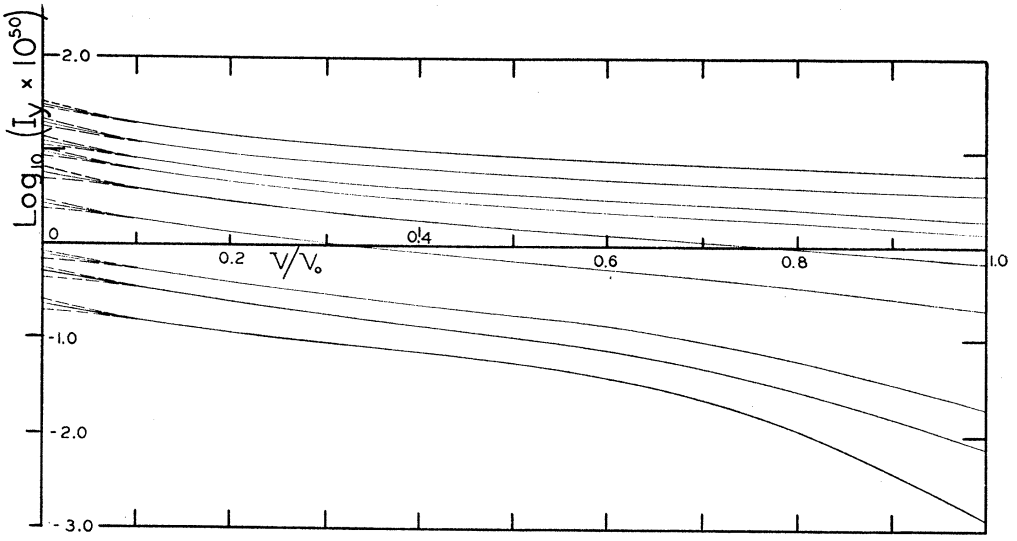

FIG. 4. Variation of I_y (or I_z) with position in the spectrum. Each curve pertains to a specific value of V/Z^2. Reading downward from the top curve, these values are 0.00985, 0.01576, 0.0272, 0.0355, 0.0613, 0.1359, 0.493, 0.790, and 1.776 electrostatic units of potential difference.

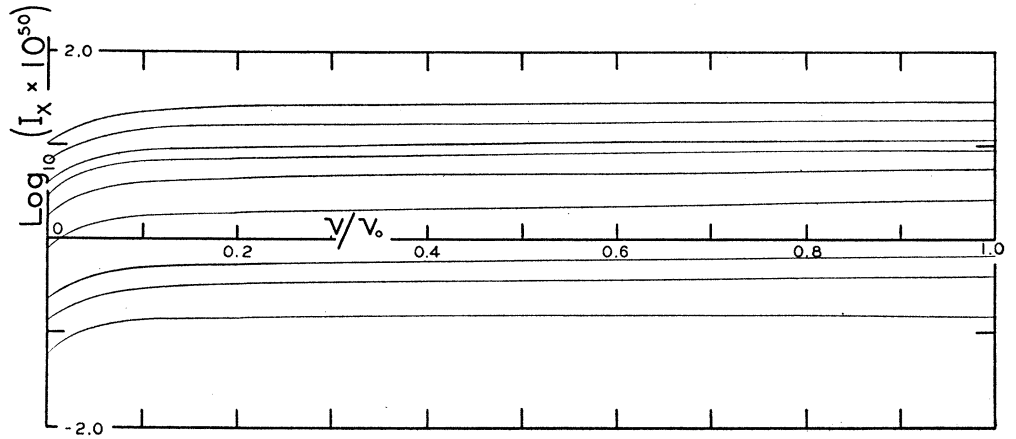

FIG. 5. Variation of I_x with position in the spectrum. Each curve pertains to a specific value of V/Z^2. Reading downward from the top curve these values are 0.00985, 0.01576, 0.0272, 0.0355, 0.0613, 0.1359, 0.493, 0.790, and 1.776 electrostatic units of potential difference.

where

$$a=1.47B-0.507A-0.833,$$

$$b=1.70B-1.09A-0.627,$$

$$A=\exp(-0.223V/Z^2)-\exp(-57V/Z^2),$$

$$B=\exp(-0.0828V/Z^2)-\exp(-84.9V/Z^2).$$

$$I'_{y,z}\times 10^{50}V/Z^2=-j+\frac{k}{(\nu/\nu_0)+h}, \qquad (9)$$

where

$$h=\frac{-0.214y_1+1.21y_2-y_3}{1.43y_1-2.43y_2+y_3},$$

$$j=(1+2h)y_2-2(1+h)y_3,$$

$$k=(1+h)(y_3+j),$$

$$y_1=0.220(1-0.390\exp(-26.9V/Z^2)),$$

$$y_2=0.067+0.023/((V/Z^2)+(0.75)),$$

$$y_3=-0.00259+0.00776/((V/Z^2)+0.116).$$

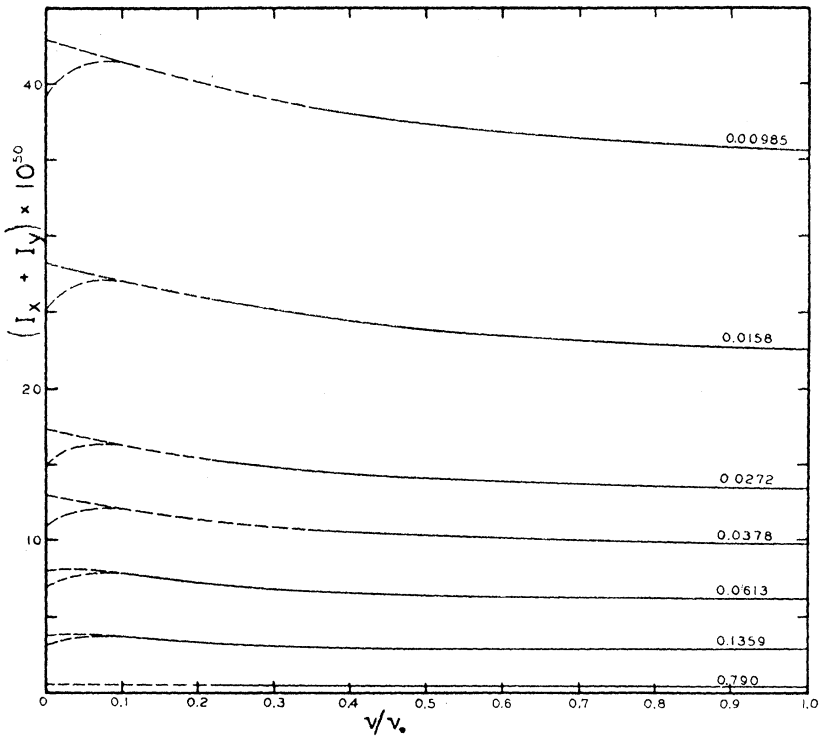

FIG. 6. Total intensity (ergs per steradian per unit frequency interval per bombarding electron per atom-per-cm²) emitted at 90° to the direction of bombardment as dependent upon position in the spectrum. Each curve pertains to the value of V/Z^2 shown just above it.

By these elementary expressions it is possible to compute the characteristics of continuous x-ray spectra with an expenditure of time and labor of the order of one percent of that required by the basic theory. Within the range covered by Table II, I_x', I_y', and I_z' differ from I_x, I_y, and I_z, respectively, by less than five percent at the worst and by about two percent on the average. The forms of Eqs. (8) and (9) have, naturally, no theoretical significance; the equations are merely empirical fits of the data of Table II.

Discussion of Table II

Figure 4, a plot of data from Table II, shows the variation of the y (or z) component of radiation with its controlling variables. In any given spectrum the component I_y (or I_z) diminishes in magnitude as the short wave limit ($\nu/\nu_0=1$) is approached. The diminution is most notable when targets of low atomic number are subject to bombardment by fast electrons. At the other end of the spectra, the Sommerfeld equations would have turned all the curves up toward infinite values. Introduction of screening in all calculations for which $\nu/\nu_0=0$ keeps the components finite but gives multiple values, since in this approximation the roles of V and Z do not always bring them together in the quotient V/Z^2. This accounts for the frayed appearance of the left-hand ends of curves of Fig. 4. It is presumed that if it were practicable to take correct account of screening throughout the spectrum, the curves of Fig. 4 would, throughout their lengths, consist of multiple bundles converging closely with increasing ν.

Figure 5 is a similar representation of I_x. The insensitivity of I_x to frequency (emphasized by logarithmic plotting) is the most conspicuous feature here. All points at $\nu=0$ have been calculated by Eq. (7), but screening has little effect on the long wave limit values of I_x and the splitting of the curves is too small to be shown.

The total radiation emitted in the direction $\theta=90°$ is given in accordance with Eq. (1) by

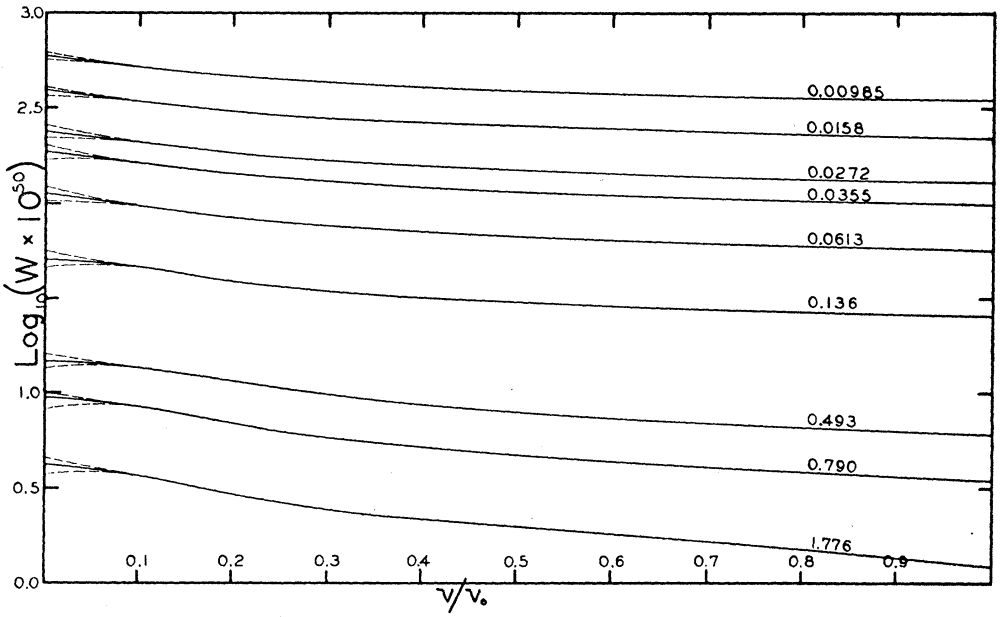

FIG. 7. Variation of total emitted energy W (in ergs per unit frequency interval per bombarding electron per atom-per-cm²) with position in the spectrum. The number immediately above each curve is the value of V/Z^2 to which the curve relates.

$I_{90°}=I_x+I_y$. Since the direction is a favorable one for observations, we show in Fig. 6 the predicted total intensities. The simplicity of these curves is remarkable. The variations of I_x and I_y with frequency, being opposite in sense, have nearly neutralized each other and given for this direction of observation a set of almost flat and linear spectra. It should be realized that these ordinates are proportional to intensities within *frequency* intervals of equal width. Most methods of spectrum observation seek to measure a quantity proportional to the intensities in *wave-length* bands of equal width, and such spectra are not flat and horizontal in character, though they may be readily transformed into a form comparable with the curves of Fig. 6.

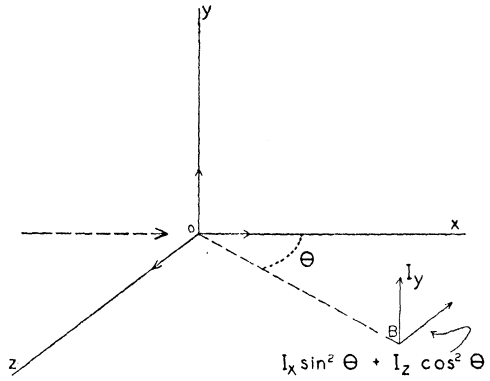

FIG. 8. Polarization components of radiation originating at 0 by bombardment from the left and observed at B.

Shifting the direction of observation to values of θ either greater or less than 90° tilts the curves of Fig. 6 so that their slight negative slopes become more accentuated and deepens their slight upward concavities.

The total radiation energy W, from Table II, is shown in Fig. 7.

POLARIZATION

In Fig. 8 the origin of radiation is O, the origin of the coordinate system, and the direction of observation is along OB, a direction specified by the angle θ. The two vectors erected at B illustrate the two components of radiation with mutually perpendicular directions of polarization. The component polarized with electric vector parallel to the y-axis of the coordinate system possesses intensity I_y; the component polarized in the perpendicular direction in general contains incoherent resolved contributions from both I_x and I_z and possesses the intensity $I_x \sin^2 \theta + I_z \cos^2 \theta$. We designate the ratio of these com-

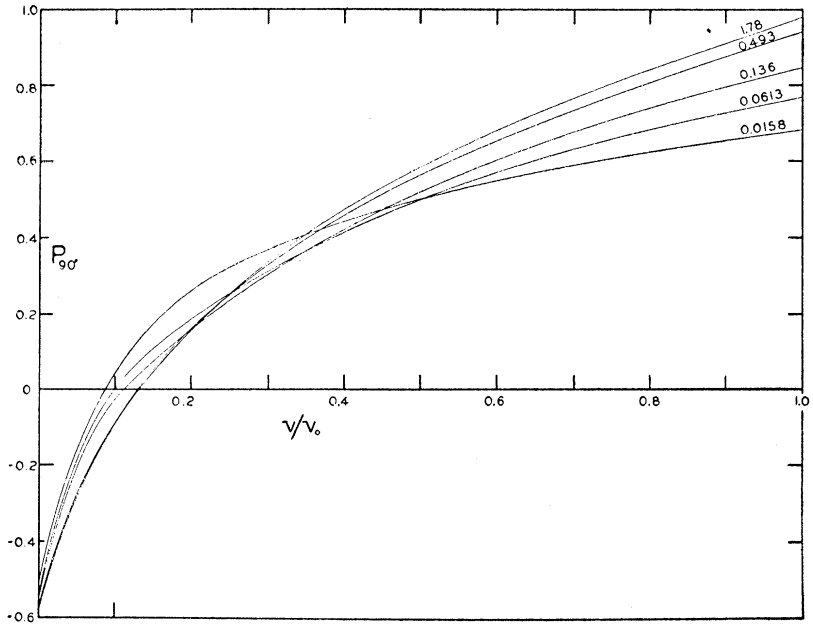

FIG. 9. Polarization of radiations emitted in a direction at 90° to the direction of bombardment. Numbers on the curves are values of V/Z^2. Scherzer investigated the case $V/Z^2=0$ and concluded that $P_{90°}=0.6$ for the entire spectrum. The curves above seem to be approaching this case as a reasonable limit.

ponents by $R=I_y/(I_x \sin^2\theta+I_z\cos^2\theta)$ and take as the measure of polarization the quantity $P_\theta=(1-R)/(1+R)$, an expression which is equivalent to $P_\theta=(1-D)/(1+D(2\csc^2\theta-1))$, where D is Sommerfeld's "depolarization ratio" I_y/I_x.

From the data of Table II, the polarization of radiation emitted in the direction $\theta=90°$ has been calculated for a number of values of ν/ν_0 and V/Z^2. These calculations are presented in the curves of Fig. 9. The similarity of these curves shows that in the present theory, polarization is more a matter of position in the spectrum than of atomic number or bombardment energy. Only in the vicinity of the short wave limit does $P_{90°}$ respond markedly to variations of V/Z^2. This response is in the sense that high V/Z^2 is associated with high (though in no case complete) polarization.

Near the low frequency end of the spectrum, radiation is produced at slight cost to the energy store of the bombardment electron. Close encounters are not required for such emission, and the predominant force component acting upon the electron lies in the yz-plane rather than the x-axis. The classical consequence, negative polarization, is supported by the curves of Fig. 9.

The curves of Fig. 9 present a somewhat tangled appearance, but they are in fact related in an entirely systematic manner, as a replot of the same data in Fig. 10 shows. The latter figure also emphasizes the relative insensitivity of polarization to V/Z^2 except in the region of low values of this quotient.

To show the theoretical variation of polarization with direction of emission, Fig. 11 is presented. Each curve here is a graph of P_θ *vs.* θ for the particular value of ν/ν_0 appended to the curve and for the value $V/Z^2=1.776$ common to all five curves. Polarization of the forward directed radiation is always zero; as θ increases, the polarization may increase or decrease, depending upon ν/ν_0. Evidently for a given V/Z^2, there is a value of ν/ν_0 for which the emitted radiation is substantially unpolarized for all directions of emission. The maximum (or minimum) of polarization at $\theta=90°$ is very flat in all cases, and observers in this angular region need have little concern about the precision of their θ measurements.

Alternative Methods of Calculation

Sauter's treatment of the problem made use of the first Born approximations. This method is

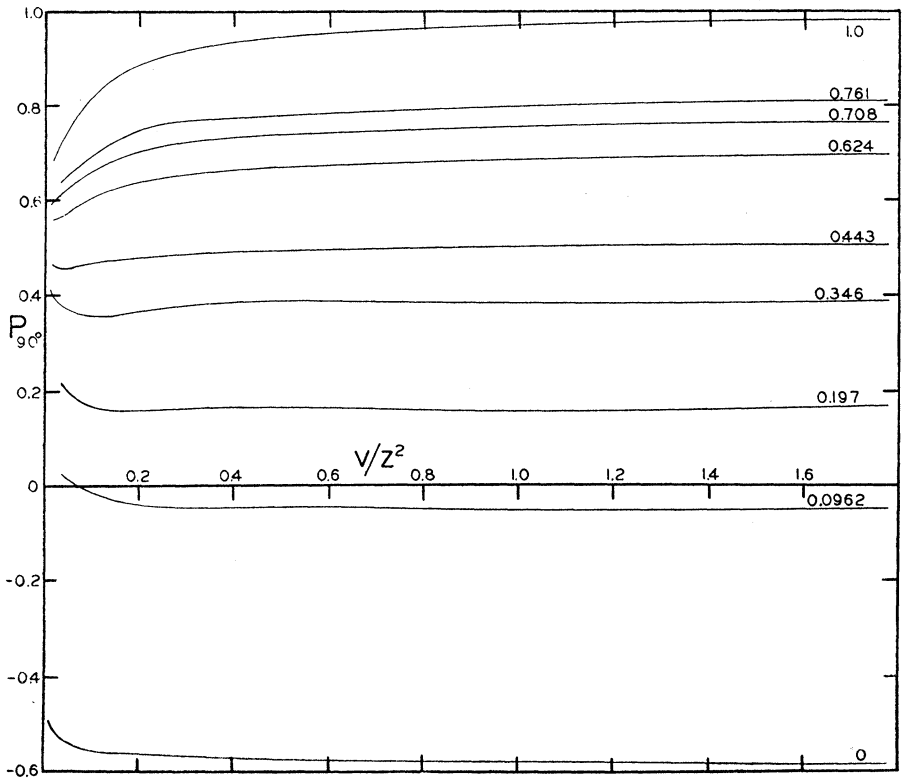

FIG. 10. Polarization of radiations emitted in a direction at 90° to the direction of bombardment. Numbers on the curves are ν/ν_0.

not appropriate unless $Ze^2/h\nu_{1,2} \ll 1$, so the method is suited only to cases in which the bombardment electron moves with high speed both before and after collision. But such cases should properly be treated relativistically and with consideration of retardation of potential.

Sommerfeld and Maue made an important contribution to the solution of the difficult problem of integrating the absolute squares of the matrix elements over all directions of electron departure when they showed that the integration necessary to the determination of the *total radiation* in all directions could be carried out exactly. The integral contains a hypergeometric function which they evaluated by an approximation which has the effect of giving spectral intensity values which are somewhat too low, as Elwert later showed. Elwert's own method undoubtedly gives a better approximation, but it is not applicable at the short wave limit since it is restricted by the condition $(Ze^2/\hbar v_2) - (Ze^2/\hbar v_1) \ll 1$, $[(|n_2| - |n_1|) \ll 1$ in Elwert's notation] while at the long wave limit, it predicts infinite intensities exactly as does the Sauter treatment.

Upon finding that the total spectral energy given by his own development exceeded that of Sommerfeld and Maue by a factor

$$\left(\frac{\sinh |n_1| \pi}{|n_1| \pi}\right)^2$$

at the long wave limit and by almost the same factor at the other extreme, Elwert conjectured that the same factor might rectify the low intensity values of Sommerfeld and Maue in all cases. This supposition was strengthened by his investigation of its effect upon a single component of the matrix elements.

We have tested this supposition by comparing certain of our own calculations (in all of which the hypergeometric function in question has been evaluated without error in excess of one percent) with corresponding intensities derived from the Sommerfeld-Maue approximation rectified by

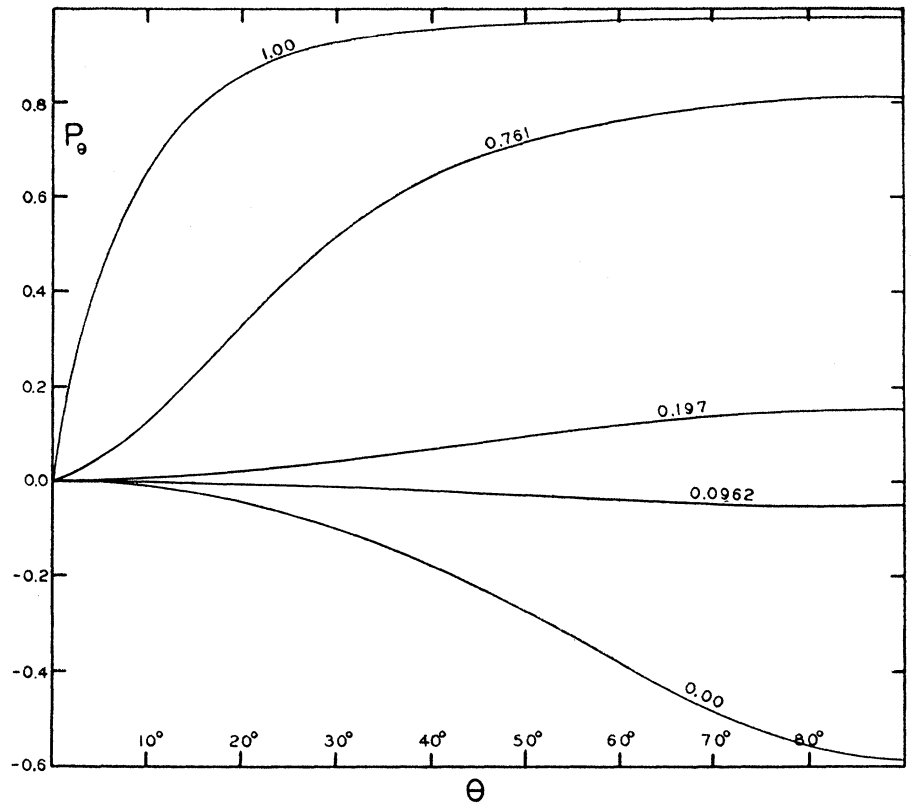

FIG. 11. Polarization *vs.* θ for $V/Z^2=1.776$ and for the values of ν/ν_0 shown on the curves. Since in the theory here considered P_θ is a function of sin θ, the curves for the next quadrant will be symmetrical continuations of those shown here.

Elwert's correction factor. Elwert's[12] statement of the Sommerfeld result is equivalent to

$$N_{sy}^2=\frac{4\pi n_1}{\xi_0^2 n_2}\{|n_1^2+n_2^2|\log(1-\xi_0)-4|n_1 n_2|\},$$

$$N_{sx}^2=\frac{8\pi n_1}{\xi_0^2 n_2}\{|n_1^2-n_2^2|\log(1-\xi_0)-4|n_1 n_2|\}.$$

The subscript s stands for Sommerfeld. Calculation of I_x, I_y, by these equations and the Elwert correction factor is exceedingly simple. Figure 12 shows that the resulting values are in good agreement with corresponding values from our Table II for the small values of $|n_2|-|n_1|$ involved in these cases. In Fig. 13 a similar comparison is made for larger values of $|n_1|-|n_2|$, and the agreement is much less good. Elwert's proposal for rectifying spectral intensities obtained under the Sommerfeld approximations is quite effective when his restricting assumption is satisfied.

[12] G. Elwert, reference 3, Eqs. (34) and (35).

Efficiency of Continuous X-Ray Production

From the radiation components of Table II, the efficiencies of continuous x-ray production in thin and thick targets may be computed. By thin target efficiency we mean the ratio of emitted x-ray energy (including all continuous spectrum frequencies and all directions of emission) to the total energy loss suffered by bombardment electrons in passing through a sample of matter so thin that only a small fraction of the electron energy is dissipated. This efficiency is not simply a function of V/Z^2, but of Z and V (or β) separately. The method of calculation in a given case is to select from Table II values of W pertaining to a common V/Z^2 but to different values of ν/ν_0 and to perform a numerical or

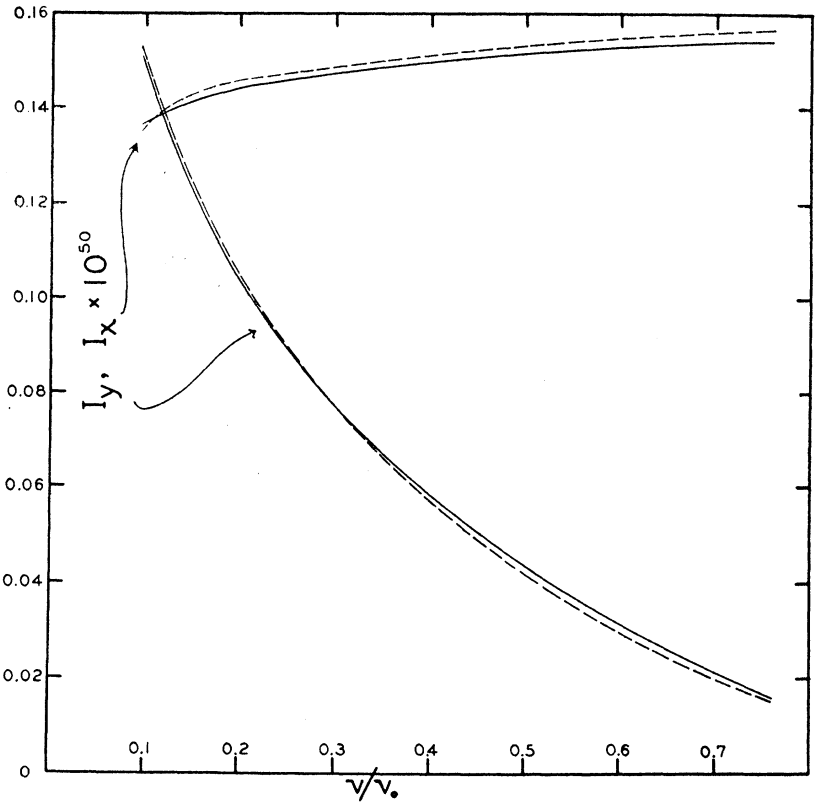

FIG. 12. Radiation components for the case $V/Z^2=1.776$. Solid curves from Table II. Broken curves by Elwert's method. Good agreement is found when $|n_2|-|n_1|\ll 1\gg|n_1|$. For these curves $0.00829<|n_2|-|n_1|<0.167$, and $|n_1|=0.160$.

graphical integration yielding the total continuous x-ray energy per electron per atom-per-cm^2

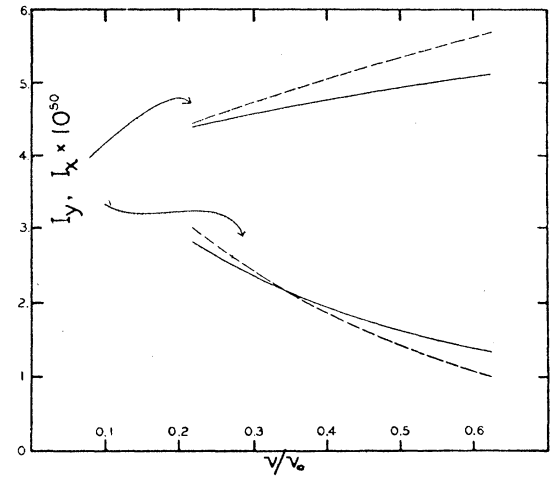

FIG. 13. Radiation components for the case $V/Z^2=0.0604$. Solid curves from Table II. Broken curves by Elwert's method, an approximation permissible only when $|n_1|\ll 1$ or $|n_2|-|n_1|\ll 1$. For these curves $0.112<|n_2|-|n_1|<0.545$, and $|n_1|=0.867$.

in all frequencies from zero to the quantum limit. It then remains to divide this result by the total energy lost per electron per atom-per-cm^2, a quantity depending upon β and Z.

In seeking the most probable values of this quantity, it seems best to adopt a combination of theoretical and experimental results. Williams[13] has shown that the observations of White[14] and Millington upon the stopping of fast β-particles by mica agree with the classical theory of Bohr[15] with respect to the functional variation of stopping power with β, though not as to the absolute values of stopping power. Williams recommends a practical formula consonant with these facts which may be put in the form:[16]

[13] E. J. Williams, Proc. Roy. Soc. **A130**, 310 (1931).
[14] P. White and G. Millington, Proc. Roy. Soc. **A120**, 701 (1928).
[15] N. Bohr, Phil. Mag. **25**, 10 (1913).
[16] An error in the statement of the energy-loss formula in Williams' Eq. (18) has been corrected above. We have also incorporated a suggestion of D. L. Webster that the right-hand side of Williams' formula be multiplied by $2Z/A$ where A is the atomic weight.

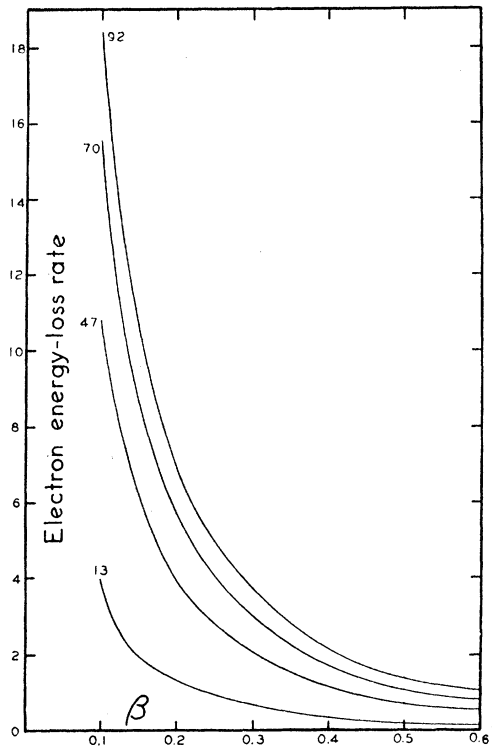

FIG. 14. Rates of loss of kinetic energy of electrons of speed β in the four substances indicated by atomic numbers near the curves. Ordinates are in ergs per atom-per-cm$^2\times10^{27}$ of stopping material. These curves are adapted from E. J. Williams' discussion of the theory of Bohr.

Energy loss in ergs per electron per atom-per-cm^2
$$=5.62Z\beta^{-1.4}\times10^{-30}. \quad (10)$$

This formula takes no account of the losses by those few collisions in which an electron loses more than 1500 kev; its applicability above $\beta=0.52$ has not been demonstrated nor has it been tested with elements of high Z. Nevertheless, we adopt it for all speeds above $\beta=0.5$ and for all elements here considered.

For low values of β (up to $\beta=0.30$) we draw upon Williams again. By cloud chamber observations of x-ray photoelectrons in oxygen, hydrogen, and argon, he established that in this energy region the Bohr theory predicts rates of energy loss about 60 percent too high, but correct in respect to their functional dependence upon Z and β. Assuming that the same ratio holds for all elements we multiply Bohr's expression by 0.6 and obtain:

Energy loss in ergs per electron per atom-per-cm^2
$$=4.07PZ\beta^{-2}\times10^{-31}. \quad (11)$$

In this equation, P is a dimensionless function of Z and V involving the geometric mean of the natural frequencies of all electrons in the atom of the stopping material. P was calculated for $Z=13$, 47, 70, and 92 by use of frequencies from the x-ray ν/R term values found in Siegbahn's *Spektroskopie der Röntgenstrahlen* (1931). Results of these calculations appear in Table IV.

To obtain electron energy losses in the region of energies intermediate between 20 and 80 kev, we have simply filled in by graphical interpolation in the manner illustrated by Fig. 14. It is gratifying that the calculations in the separated ranges admit of a smooth connecting curve segment for each of the four elements used in these efficiency calculations. We do not take this to mean that these curves are entirely correct; they may be wrong by many percent, but they would seem to be as good approximations as the literature of the subject affords at this date. Our efficiency conclusions will be subject to immediate amendment upon the appearance of more reliable energy-loss information. Figure 14, showing the energy-loss rates which we have adopted, may be used as a basis for any such adjustment.

TABLE IV. Electron-loss rates from Eq. (11).

Z	β	Kilovolts	P	Loss rate $\times10^{28}$
13	0.10	2.57	7.47	39.5
13	0.15	5.84	8.38	19.7
13	0.20	10.53	9.97	13.2
13	0.25	16.75	10.77	9.12
13	0.30	24.66	11.43	6.72
47	0.10	2.57	5.66	108.2
47	0.15	5.84	7.12	61.0
47	0.20	10.53	8.15	39.0
47	0.25	16.75	8.96	27.4
47	0.30	24.66	9.61	20.4
70	0.10	2.57	5.46	155.5
70	0.15	5.84	6.92	87.6
70	0.20	10.53	7.95	56.7
70	0.25	16.75	8.76	39.9
70	0.30	24.66	9.41	29.8
92	0.10	2.57	4.91	183.8
92	0.15	5.84	6.42	106.8
92	0.20	10.53	7.40	69.3
92	0.25	16.75	8.21	49.2
92	0.30	24.66	8.86	36.9

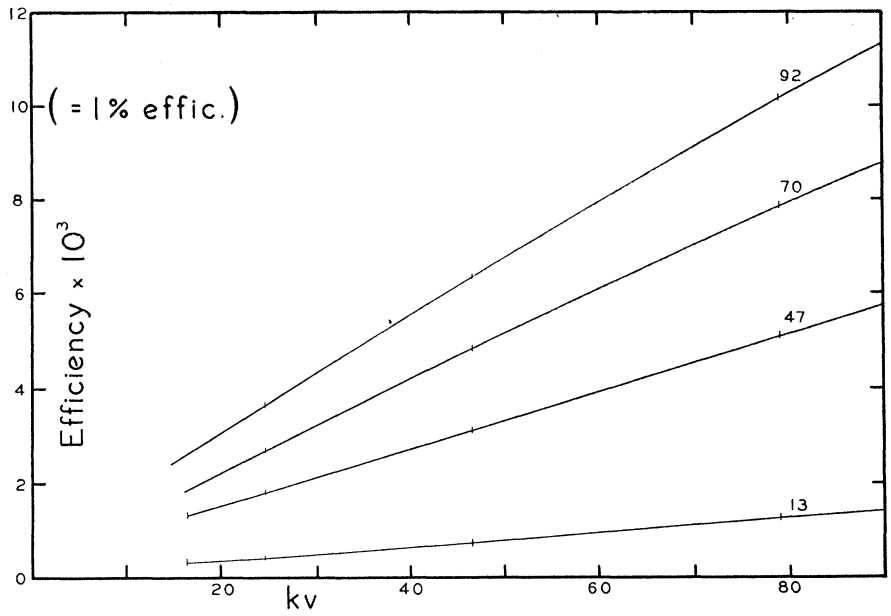

FIG. 15. Efficiency of production of continuous x-rays by thick targets of atomic numbers shown beside the curves when bombarded by electrons at the stated kv values. Curves are based on electron energy-loss rates of Fig. 14 and theoretical continuous spectrum energies derived from Table II. Approximate proportionality of efficiency to bombardment energy is shown.

The thin target efficiencies are given in Table V along with thick-target efficiencies now to be explained.

If E represents the varying kinetic energy of a typical electron slowing down from E_0 to zero in a thick target, then R, the output of x-ray energy, is given by

$$\int_0^{E_0} (dR/dE)dE,$$

TABLE V. Calculated efficiencies of continuous x-ray production in thin and thick targets of atomic number Z. For thin targets kev denotes the energy of bombardment at the point of production. For thick targets it denotes the energy at incidence upon the target.

kev	$Z=13$	$Z=47$	$Z=70$	$Z=92$	
15	5.3	23.0			thin target efficiencies $\times 10^4$
25	7.9	34.0	50.0	69.0	
40	13.0	53.0	80.0	110.0	
90	27.0	110.0	160.0	210.0	
16.8	3.4	14.0			thick target efficiencies $\times 10^4$
24.7	4.4	18.0	28.0	37.0	
46.5	7.6	32.0	48.0	64.0	
79.0	13.0	51.0	79.0	100.0	
90.0	15.0	58.0	88.0	110.0	

where the derivative in parentheses is just the thin target efficiency. It is convenient to perform the graphical integration with respect to β, in which case we have

$$R=\int_0^{\beta_0} (dR/dE)(dE/d\beta)d\beta.$$

The second of the derivatives in the integrand is obtained by differentiating the relativistic expression for electron kinetic energy in terms of β. The integration has been carried out for twenty representative cases, and the over-all thick target efficiencies of continuous x-ray production have been obtained by dividing R by the initial electron energy. These efficiencies are shown in Table V, and Figs. 15 and 16.

From direct measurement of the x-ray and cathode ray energies Beatty[17] found thick target efficiencies to be proportional to the product of target atomic number and bombardment voltage. The many efficiency measurements made subsequently to Beatty's time were summarized by

[17] R. T. Beatty, Proc. Roy. Soc. 89, 314 (1913).

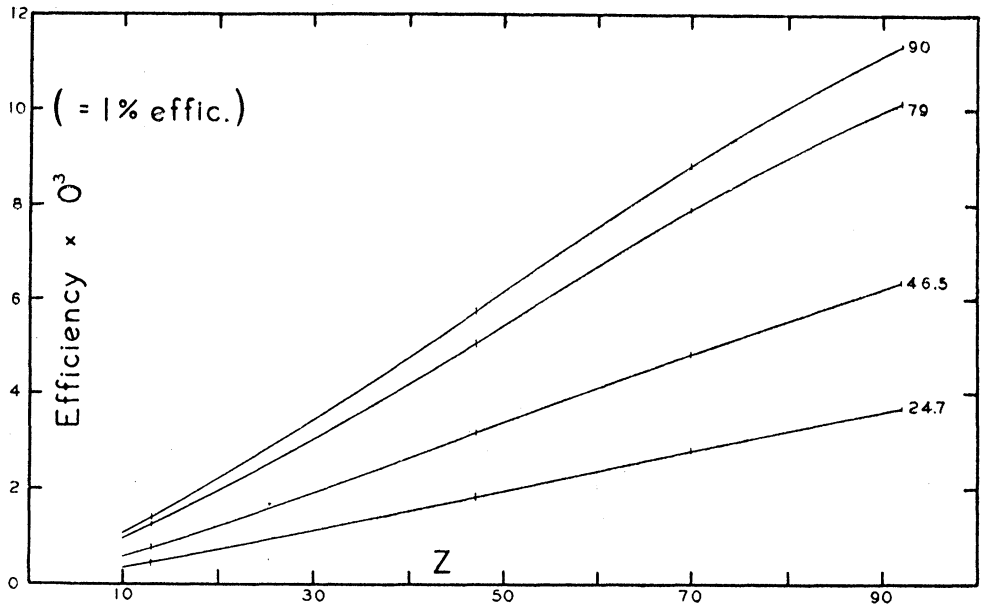

FIG. 16. Efficiency of production of continuous x-rays by thick targets of atomic numbers shown by the ordinate scale when bombarded by electrons at the kv values stated at the ends of the curves. Curves are based on electron energy-loss rates of Fig. 14 and theoretical continuous spectrum energies derived from Table II. Approximate proportionality of efficiency to atomic number is shown.

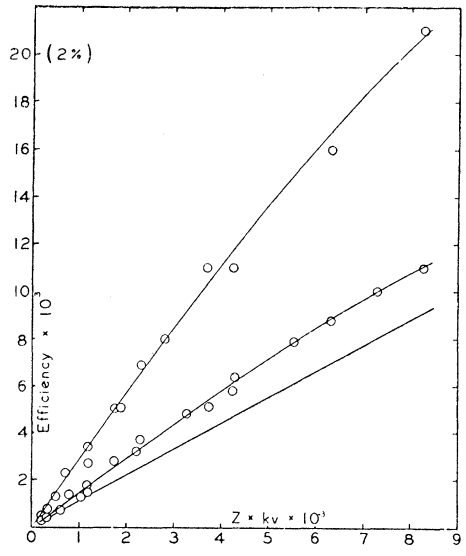

FIG. 17. Calculated efficiency of production of continuous x-rays in thin targets (upper curve) and thick targets (middle curve) of atomic number Z bombarded by electrons accelerated by potential kv. Approximate linearity of thick target curve supports Beatty's rule. Failure of points to lie precisely on the curves shows that efficiencies as here calculated are not strictly functions of the product Z kv. The lower curve is a consensus of the experimental results of several investigators of thick-target efficiency.

Compton and Allison[18] in the equation Efficiency $=1.1\times10^{-6}Z$ kv, a summary which these authors regarded as "probably correct within about 20 percent."

Figure 17 shows that the efficiencies of Table V[19] agree approximately with Beatty's rule and that they lie about 20 percent above the values of the consensus of Compton and Allison.

For any product Z kv the calculated thin target efficiency is about twice as great as the thick target efficiency. The thin target points in Fig. 17 are tolerably represented by the straight line

$$\text{Thin target efficiency} = 2.8\times10^{-6}Z \text{ kv}.$$

Calculated efficiencies for both thin and thick

[18] A. H. Compton and S. K. Allison, *X-Rays in Theory and Experiment* (D. Van Nostrand Company, Inc., New York, 1935), p. 90.

[19] The efficiencies of Table V lie somewhat below the values given earlier by one of the present authors (P. Kirkpatrick, Phys. Rev. **66**, 156 and 161 (1944)). The original calculations were based upon the energy-loss rates of Eq. (10) for low voltages as well as high. The values of W at $\nu=0$ in the previous work were obtained by graphical extrapolation instead of direct calculation. Changing the method of calculation in these two respects produced efficiencies more precisely proportional to Z and kv and, on the whole, lower,

targets tend to fall below linearity at high values of Z kv, but the reliability of the calculations is in question here since the potentials involved are outside the proper range of non-relativistic theory.

Dr. Robert Weinstock assisted the authors through numerous discussions in the early stages of the work, when his interpretation of his own papers contributed most helpfully to the development of the computational procedure.

PHYSICAL REVIEW VOLUME 67, NUMBERS 11 AND 12 JUNE 1 AND 15, 1945

The Relativistic Correction in the Meson Theory of Nuclear Force

NING HU
Institute for Advanced Study, Princeton, New Jersey
(Received March 23, 1945)

In the present paper a systematic investigation is made on the relativistic corrections of the usual non-relativistic meson theories of nuclear force by expansion with respect to the dimensionless operator ∇/M. The mixed theory initiated by Møller and Rosenfeld is considered since it is the only satisfactory theory in the non-relativistic region. It is found that the inadmissible singularity which has been removed in the mixed theory in the non-relativistic region reappears in the higher approximations. This means that the extension of the mixed theory to the relativistic region as done by Møller and Rosenfeld in explaining the quadrupole moment is not justified.

I. INTRODUCTION

THE well known fact that the deuteron nucleus possesses an electric quadrupole moment is an indication of the existence of the tensor force in the nuclear interaction. The expression for this force derived from a single type of meson field, however, contains the inadmissible singularity of the type $1/r^3$, which has to be cut off at an arbitrary radius. It has been shown by Møller and Rosenfeld[1] that if the nuclear interaction is assumed as due to a mixed field of pseudoscalar and vector mesons of the same mass and suitably chosen coupling constants, then the tensor force disappears with its inadmissible singularity in the non-relativistic region. This provides a solution of the wave equation without resorting to the cut-off procedure. According to this theory, the quadrupole moment can only be a relativistic effect owing to the vanishing of the tensor force in the non-relativistic region. Møller and Rosenfeld have actually derived an expression for the quadrupole moment by considering the relativistic interaction of the first order. Schwinger[2] later suggested that if the mass of the vector meson is assumed to be larger than that of the pseudoscalar meson, then the tensor force reappears with an admissible singularity of the type $1/r$. This assumption is also in agreement with the hypothesis that the vector meson is highly unstable and responsible for the β-disintegration of the nucleus.

Recently Jauch and the present author[3] calculated numerically the quadrupole moment according to Schwinger's assumption, and found that the result is much smaller than the experimental value even for a very large mass ratio for these two types of mesons. This conclusion is quite independent of the coupling constants obtained from the scattering problems. Parallel to this calculation, Hulthén[4] also evaluated the quadrupole moment using the formula obtained by Møller and Rosenfeld. The

---

[1] C. Møller and L. Rosenfeld, Kgl. Danske Vid. Sels. Math.-Fys. Medd **17** (1940).
[2] J. Schwinger, Phys. Rev. **61**, 287A (1942).
[3] J. M. Jauch and N. Hu, Phys. Rev. **65**, 289 (1944).
[4] L. Hulthén, Arkiv for Mat. Astr. Och. Fys. **29A**, No. 33 (1943).